International Journal of Applied Chemistry.
ISSN 0973-1792 Volume 12, Number 3 (2016) pp. 399-409

http://www.ripublication.com

Characterization and Photocurrent Response of Mn-N-TiO_2/Ti Electrode : Approach for Chemical Oxygen Demand (COD) Sensor

Ruslan[1]*, Mohamad Mirzan[1], Muhammad Nurdin[2]* and Abdul Wahid Wahab[3]

[1]Departement of Chemistry, Faculty of Mathematics and Natural Sciences, Tadulako University, Jl. Soekarno-Hatta 94118, Palu-Indonesia.
[2]Department of Chemistry, Faculty of Mathematics and Natural Sciences, Universitas Halu Oleo, Jl. HEA Mokodompit Anduonohu 93232, Kendari-Indonesia.
[3]Department of Chemistry, Faculty of Mathematics and Natural Sciences, Hasanuddin University, Jl. Perintis Kemerdekaan 90245, Makassar-Indonesia.

Abstract

The preparation of a thin film of nano-sized Mn-N-TiO_2, attached to a substrate Ti plate, was carried out. This preparation was performed by dip-coating in a sol-gel, refluxing, and then calcining at 450°C. The Mn-N-TiO_2 crystals were characterized by DRS, XRD, FTIR, SEM, and BET. The Mn-N-TiO_2/Ti film was characterized by a potentiostat. The results of the DRS measurements indicated that the wavelengths were in the visible region. The XRD measurements showed that the product was dominated by Mn-N-TiO_2 in the anatase form, with a crystallite size of 15.43 nm. Characterization by FTIR indicated the presence of Ti-O, -NO, Ti-N and Mn-O bonds. BET analysis the pore surface area, pore volume, and pore were 92.95 m^2/g, 0.03 cm^3/g, and 5.5 Å, respectively. The SEM measurements showed that the crystals were small in size and well dispersed. Photocurrent response of Mn-N-TiO_2/Ti electrode was active in absorbing the visible light. This system can be used as a sensor for COD.

Keywords: Nitrogen, Manganese, Titanium dioxide, Degradation, Visible.

INTRODUCTION

The limitations of the conventional methods for determining the COD (chemical oxygen demand) have led to many attempts by researchers to overcome the shortcomings that exist [1]. The development of COD determination methods can be classified into two categories [2]. The first includes conventional methods, which involve the principle of chemical oxidation [3]. The second includes methods that involve electrocatalytic oxidation to measure the COD value [4].

Similarly, methods for organic waste management are being developed at this time that are based on photodegradation [5,6]. In addition to being more effective, the method is considered more operationally economical. Through this method, waste containing large quantities of organic compounds undergoes decomposition, so that its toxicological effects on the environment are reduced [7]. In fact, the ideal degradation of hydrocarbons produces only carbon dioxide and water, and therefore has no unwanted side-effects and necessitates no further treatment [8,9].

This has encouraged scientists to create an innovation-friendly environment, introducing the principle of optimization and efficiency of industrial processes, which has come to be known as the concept of green chemistry [10,11]. Since the publication of the phenomenon of photocatalytic titanium dioxide by Fujishima and Honda i.e. the splitting of water into oxygen and hydrogen by semiconducting TiO_2 under ultraviolet light, materials based on TiO_2 have been studied to address environmental problems [12].

Various attempts have been made to obtain high photocatalytic efficiency, including the synthesis of nano-crystalline TiO_2, the insertion of dopants, and the addition of sensitizers [13-15]. Various forms of photocatalytic reactors have been designed and applied to the degradation of organic substances in the liquid or gas phase [16,17]. Some researchers have carried out modifications of the photocatalyst matrix of TiO_2 to allows its activation by visible light. One form of modification is the insertion of other atoms (dopants) into the TiO_2 crystal matrix, wherein the matrix elements of the dopant create a new catalyst that has a smaller band gap value equivalent to the energy of visible light [18,19].

Efforts to use Mn and N as dopants, which function to extend the photocatalytic activity of TiO_2 to visible light radiation for COD sensing and for the degradation of dyes, have not been widely studied. In this study, TiO_2 will be modified with the non-metal dopant N (nitrogen) and the metal dopant Mn on a Ti plate substrate. The addition of the dopants Mn and N in the TiO_2 catalyst system is expected to improve the performance of the reform-photocatalytic process [20,21] in its application for the measurement of COD and the degradation of a dye triggered by irradiation in the visible light region [22]. The addition of Mn and N as dopants may also serve as the active core of the TiO_2 photocatalytic process, as well as electron traps to prevent electron–hole recombination [23]. Thus, it may improve the performance of the photocatalytic degradation of dyes in wastewater.

The photoactivity of the synthetic product will be evaluated by measuring its ability to photocatalytically degrade wastewater produced by the textile industry [7]. The selection of the textile industry for the wastewater system was based on the abundance of organic compounds, and the simulation based on this system is expected to yield a photocatalytic application in industrial waste management techniques [6]. The photodegradation parameters will be determined by the results of the characterization of the synthetic Mn-N-TiO_2 product.

The main feature of the development of the photoelectrochemical cell system is the preparation of the nano-sized Mn-N-TiO_2/Ti film in order to obtain a film anode having a large surface area and high activity. The sol-gel method and calcination will be used to prepare the Mn-N-TiO_2 film as desired. This paper will report the results of the characterization of the produced Mn-N-TiO_2 film, which will be used as the working electrode in the measurement of the pollutant degradation of COD and dye-based photoelectrochemistry.

RESEARCH METHODS

Material

The materials used in this study were titanium tetraisopropoxide (TTIP; 97%, Aldrich), ethanol (95%), $NaNO_3$ (0.1 M), distilled water, HCl (31%), HF (40%), HNO_3, acetylacetonate, urea, a Ti plate, and NH_3, 2-propanol, acetic acid, $MnCl_2.2H_2O$.

Synthesis of Mn-N-TiO_2 Sol-gel Method

The initial step in the synthesis of Mn-N-TiO_2 by the sol-gel method was to prepare a mixture of two solutions. The "A" solution, a TiO_2 colloidal solution, was prepared by the controlled hydrolysis of TTIP (4 mL) in 0.5 mL of acetylacetonate and 15 mL of ethanol or 2-propanol in a reflux flask. The "B" Solution was prepared by placing 15 mL of ethanol and 2 mL of distilled water, with the addition of 1 mL of 0.5 M acetic acid, into a separating funnel. Then, the "B" solution was added to the "A" solution gradually through the funnel while stirring using a magnetic stirrer. The solution mixture was refluxed for 2 hours at 50°C.

A sol of TiO_2 was obtained in a beaker glass, to which was added $MnCl_2 \cdot 2H_2O$ (varying the concentration of the metal ion Mn to 1%, 2% and 3% by weight). The mixture was stirred magnetically for 3–4 hours to obtain a homogeneous mixture. The next step was performed in order to dope Mn-TiO_2 with a source of nitrogen (urea). The same sol was stirred using a magnetic stirrer, followed by the addition of the nitrogen source at concentrations of 1.0, 1.50 and 2.0 M for 1 hour at 50°C to produce a Mn-TiO_2 sol containing nitrogen.

The sol was oven-dried at a temperature of 80°C for 30 minutes and calcined at a temperature of 500°C for 2 hours. A powder of Mn-N-TiO_2 was obtained, ready for characterization by UV-Vis diffuse reflectance spectroscopy (UV-Vis DRS), X-ray diffraction (XRD), Fourier transform infrared spectroscopy (FTIR), scanning electron microscopy (SEM) and Brunauer–Emmett–Teller (BET) analysis.

Preparation of Electrode

a. Ti Plate

A Ti plate, which had been previously prepared, was then immobilized by sols of TiO_2, N-TiO_2, Mn-TiO_2 and Mn-N-TiO_2 by superimposing the plate surface evenly using a deep coating technique. Then, the plate was allowed to dry and calcined in a furnace at a temperature of 500°C for 3 hours to allow the formation of anatase crystals, which progressed well. In order to obtain a uniform thin film on the surface of the plate, the coating process was repeated three times.

Characterization of Mn-N-TiO_2 Catalyst

Characterization was performed to determine whether the products were in accordance with the intended purpose. The products, including the synthesized TiO_2 and N-doped TiO_2 and the films of TiO_2 and N-doped TiO_2, were found to have been prepared successfully. The synthesized Mn-N-TiO_2 was characterized using UV-Vis DRS, XRD, SEM, FTIR and BET, while the Mn-N-TiO_2 films were characterized using an electrochemical system or a potentiostat.

RESULTS AND DISCUSSION

Characterization by UV-Vis DRS

Characterization of Mn-N-TiO_2 was conducted by UV-Vis DRS to obtain information about the crystal band gap of the electrodes. The overall results of the analysis of TiO_2, N-TiO_2, Mn-TiO_2 and Mn-N-TiO_2 are shown in Table 1.

Table 1. Measured band gap energies of TiO_2, N-TiO_2, Mn-TiO_2 and Mn-N-TiO_2

No.	Sample	Gap energy (eV)
1.	TiO_2 Degussa P-25	3.35
2.	TiO_2 pH 3	3.20
3.	N-TiO_2	3.03
4.	Mn-TiO_2	2.32
5.	Mn-N-TiO_2	2.22

From Table 1 it can be seen that the band gaps of N-TiO_2, Mn-TiO_2 and Mn-N-TiO_2 are lower than that of TiO_2 in the visible light region. The band gap can be used to calculate the corresponding wavelength by the following formula:

$$Eg = \frac{hc}{\lambda g} = \frac{1239.8}{\lambda g} = (eV)$$

With decreasing values of the band gap, the energy of light required to form the photohole (conduction band) and photoelectron (valence band) will decrease, conceivably allowing the use of a visible light source.

Characterization by XRD

Characterization by XRD was performed to obtain information about the crystal structures of the synthesized TiO_2, N-TiO_2, Mn-TiO_2 and Mn-N-TiO_2. The XRD analysis of the materials was conducted using calcined gels, which were not coated on a Ti plate substrate, but received the same heat treatment as those that were coated on a substrate.

Figure 1 shows the results of the XRD analysis of the TiO_2, N-TiO_2, Mn-TiO_2 and Mn-N-TiO_2 catalysts. In the figure, peaks can be seen that provide information about the identity of the crystalline forms prepared in this study. The crystal forms can be determined by comparing the values of 2θ or *d* (Å) from the measurements with the standard card data for crystalline TiO_2.

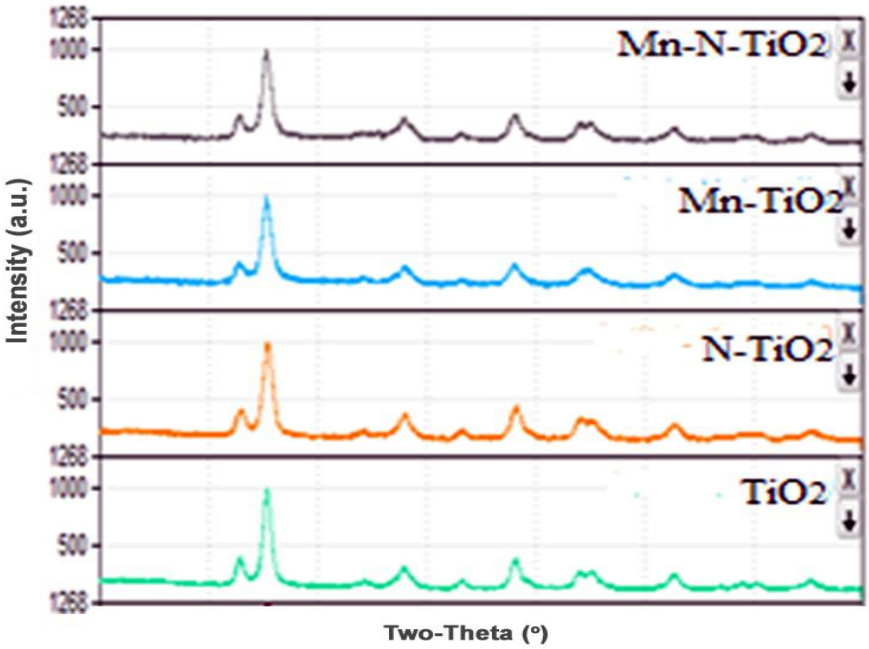

Figure 1. XRD analysis of TiO_2, N-TiO_2, Mn-TiO_2 and Mn-N-TiO_2

The XRD analysis results for the TiO_2 catalyst are shown in Figure 1. It can be seen that the XRD pattern contains nine peaks of diffraction at 2θ = 25.39°, indicating that the samples of TiO_2, N-TiO_2, Mn-TiO_2 and Mn-N-TiO_2 were dominated by crystalline anatase. From the peaks of the diffractograms, it was calculated by the Scherrer equation that the crystal size was 17.89 nm for the TiO_2 catalyst and 15.43 nm for the Mn-N-doped TiO_2 catalyst.

Characterization by FTIR

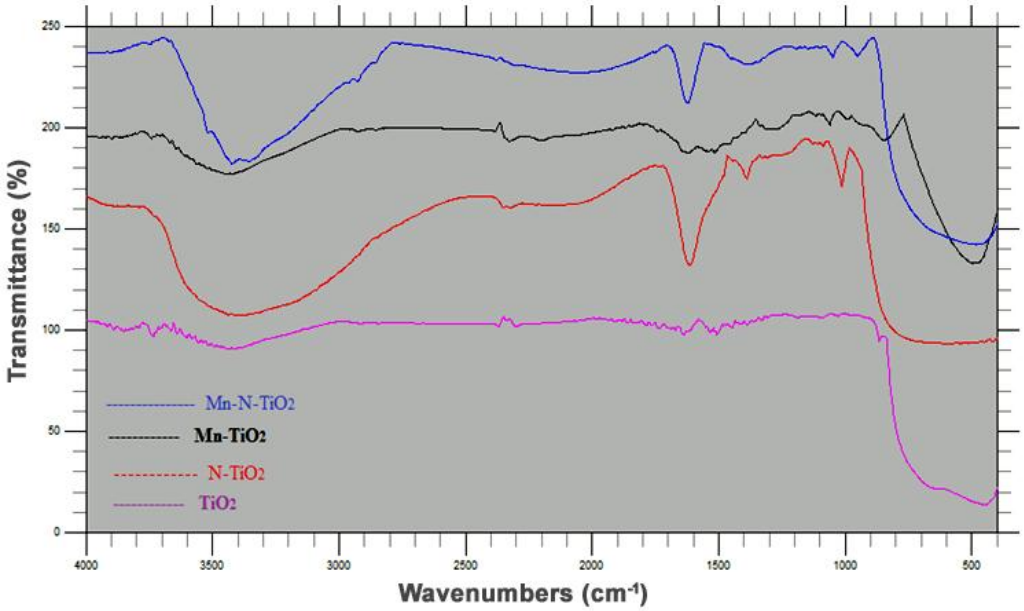

Figure 2. FT-IR spectra of TiO_2, N-TiO_2, Mn-TiO_2 and Mn-N-TiO_2

The spectra obtained by characterization using FTIR are shown in Figure 2. This indicates the presence of -OH stretching, marked by the appearance of absorption peaks at around 910 cm^{-1} (bending vibration) with a weak signal, and 3400 cm^{-1} (stretching vibration) with a strong signal. The presence of OH groups arises from the titanyl groups at the Ti-OH terminus of the crystal phase of TiO_2 and water adsorbed on the surface. The indication of the presence of the stretching of CN groups probably arises from aliphatic amine groups, which are characterized by the presence of a peak at around 1064 cm^{-1}. In addition, the presence of the C=O stretching indicated by the absorption peak at 1600 cm^{-1} is derived from ketone groups [22].

An indication of the presence of Ti-O bonds occurs in the absorption peak at 600 cm^{-1}, while the absorption peak at 1475 cm^{-1} (symmetric vibration) indicates the presence of –NO groups. This absorption provides evidence of the insertion of nitrogen into the TiO_2 matrix. In addition, an indication of the presence of Ti-N bonds occurs in the absorption peak at 508 cm^{-1}, with a weak signal. The amount of nitrogen present in the catalyst is evidently low.

Characterization of the functional groups in the Mn-TiO_2 composite was performed using an FTIR in the wavenumber range of 400–4000 cm^{-1}. The strong, broad absorption peaks at the wavenumbers 3394.72 and 1620.21 cm^{-1} are the O-H stretching and bending vibrations of H_2O molecules trapped within the framework of the hygroscopic composite. The Ti-O peak of TiO_2 appears at 2337.72 cm^{-1}. The influence of the atomic mass of Mn on the Ti-O bonds can be calculated by Hooke's Law: the greater the mass of the atoms interacting, the lower the frequency of

vibration, hence the smaller the wavenumber [24]. From the decline in the absorption wavenumber of the composite TiO_2 from 1064.71 to 1056.99 cm^{-1}, it is evident that the metallic Mn ions were immobilized. It is thus concluded that the composite Mn-N-TiO_2 had been successfully synthesized.

Characterization by SEM

The SEM measurement results provide information about the surface topography of the crystals.

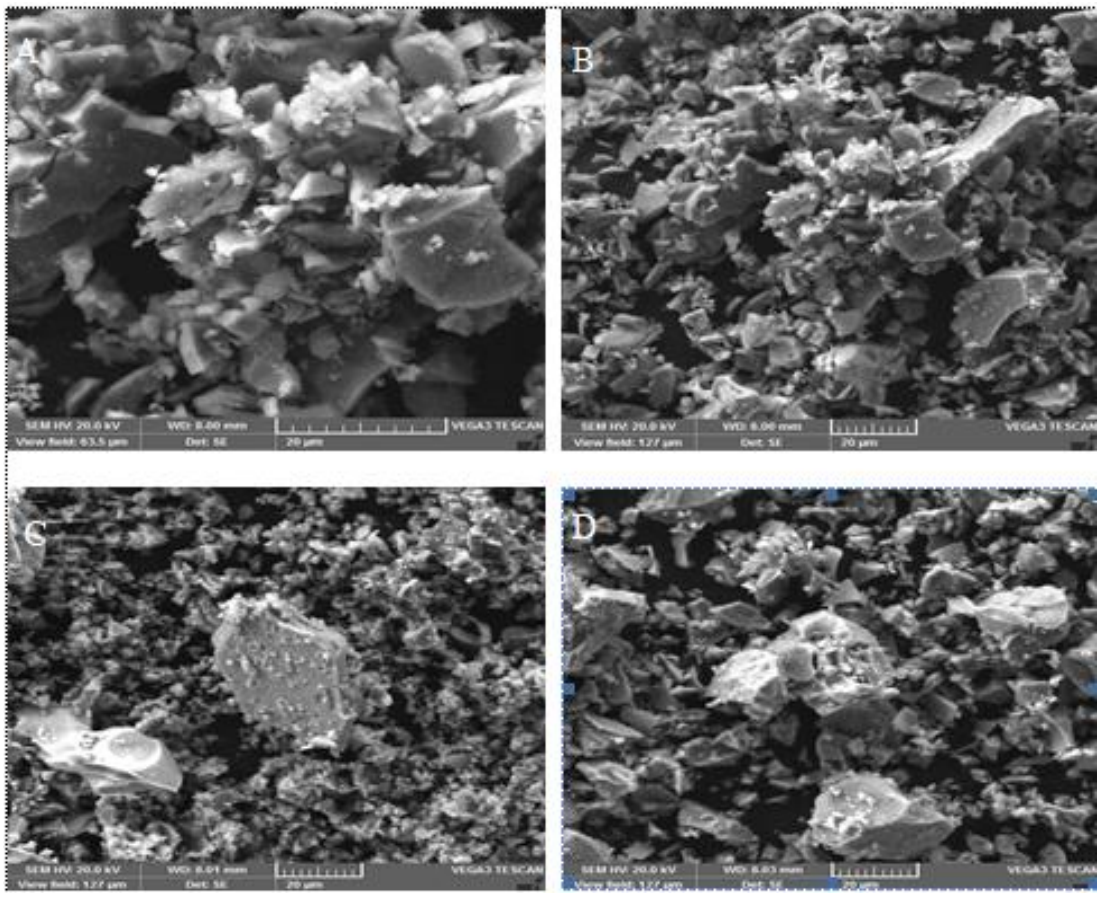

Figure 3. SEM characterization: A.TiO_2, B. N-TiO_2, C. Mn-TiO_2 and D. Mn-N-TiO_2

It can be seen in Figure 3 that the crystals are very small in size, and well dispersed, although some agglomerations are also present. These may be caused by the presence of solvent molecules trapped in the crystal structure of TiO_2. This is consistent with the appearance of the peak related to the O-H vibration in the FTIR spectra presented above. The small crystal size enhances the activity of the catalyst: because the photocatalysis takes place on the surface of the catalyst, the smaller the particle size, the greater the active surface area that is exposed to the substrate, thus accelerating the photocatalytic reaction [25].

Analysis of Pore Surface Area (BET)

Characterization was performed using a surface area analyzer to determine the surface area, pore volume and pore diameter of the composites TiO_2 and Mn-N-TiO_2. This determination was based on the absorption of nitrogen gas by the surfaces of the porous solids, as modeled by BET theory. The BET surface areas of the composites TiO_2 and Mn-N-TiO_2, as well as the obtained porosity curves for the isothermal adsorption/desorption of nitrogen gas (N_2) by the composites, are shown in Figure 4.

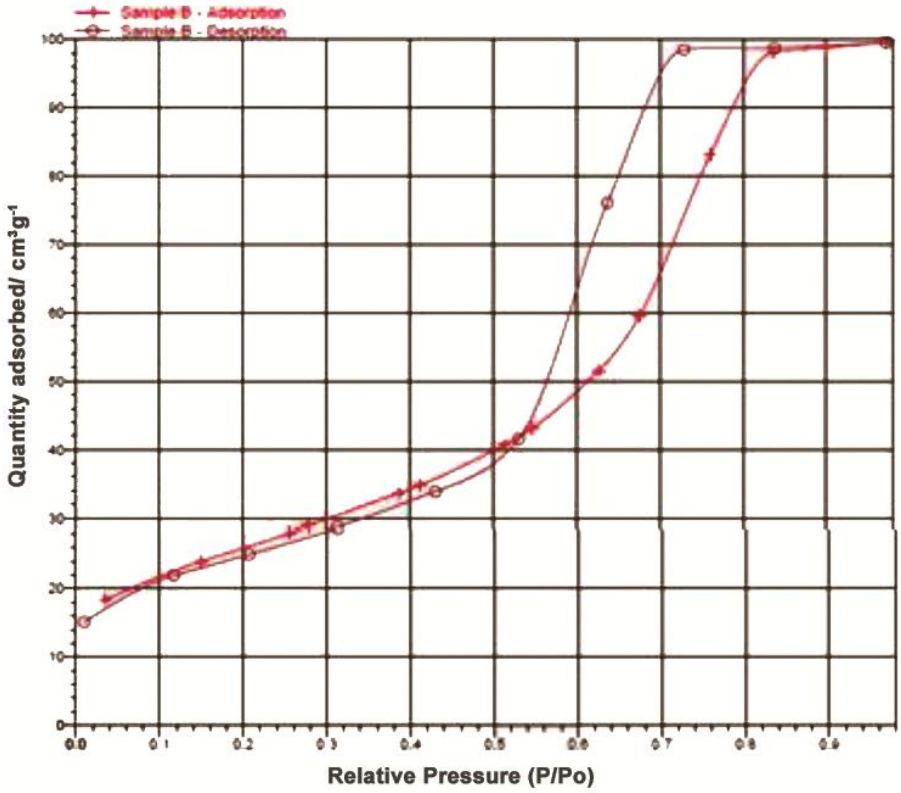

Figure 4. Isothermal adsorption/desorption of N_2 gasses

Based on analysis of the BET results, the addition of Mn and N into the composite TiO_2 caused an increase in the pore surface area from 55.74 to 92.95 m^2/g, a decrease in the pore volume from 0.10 to 0.03 cm^3/g, and a decrease in the pore diameter from 6.0 to 5.5 Å.

The increase in the surface area of the composite Mn-TiO_2 is thought to originate from the immobilization of the transition metal Mn ions and non-metallic N ions on the composite structure of Mn-N-TiO_2, causing increased breaking of the surface. The immobilization of Mn and N on the TiO_2 framework leads to changes in the bonding, making the structural arrangement of the atoms less regular, so that the surface area increases. The surface area of the composite Mn-N-TiO_2 plays an important role in photocatalysis by visible light. Additionally, the adsorption of the substrate on the catalyst surface is a requirement for the photodegradation process; therefore, the

larger surface area of the photocatalytic composite is desirable because it facilitates the adsorption of organic matter and allows the transfer of the adsorbate compound to the active site.

Photocurrent Response of Electrode Modification Mn-N-TiO2/Ti

Measurements of photocurrent response to Mn-N-TiO2/Ti electrode was performed using UV and Visible lights irradiation as well as measurement in the dark condition (Figure 5).

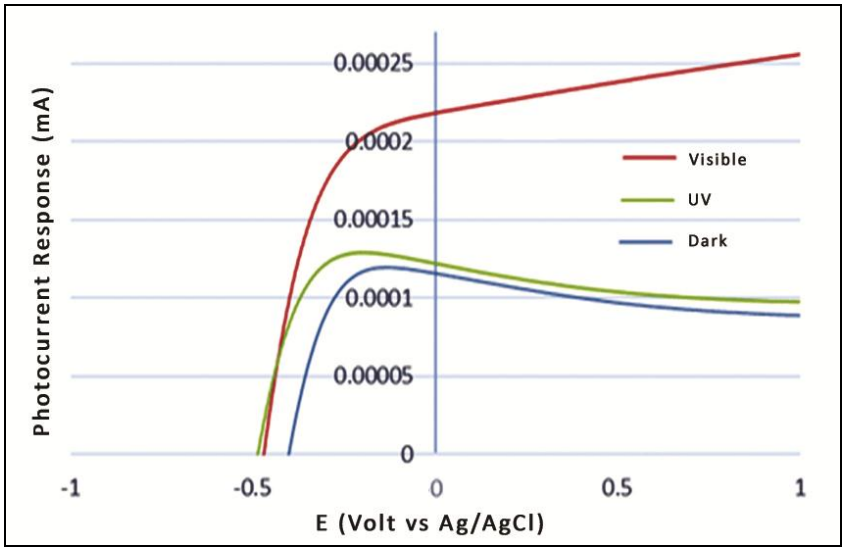

Figure 5. Photocurrent measurement of Mn-N-TiO2/Ti.

It shows that the largest photocurrent response is shown visible light response. The photoactive in visible light prove that the addition of Mn and N was able to create an active catalyst in absorbing the visible light. This system can be used as a sensor for COD, and for the degradation of dyes in the visible light region.

CONCLUSION

DRS measurements indicated that the wavelengths were in the visible region. The XRD measurements showed that the product was dominated by Mn-N-TiO_2 in the anatase form, with a crystallite size of 15.43 nm. Characterization by FTIR indicated the presence of Ti-O, -NO, Ti-N and Mn-O bonds. The SEM measurements showed that the crystals were small in size and well dispersed. Based on analysis of the BET results, the addition of Mn and N into the composite TiO_2 caused an increase in the pore surface area from 55.74 to 92.95 m^2/g, a decrease in the pore volume from 0.10 to 0.03 cm^3/g, and a decrease in the pore diameter from 6.0 to 5.5 Å. The photoactive in visible light prove that the addition of Mn and N was able to create an active catalyst in absorbing the visible light.

ACKNOWLEDGEMENT
We acknowledge for financial support of the DRPM-Ministry of Research, Technology and Higher Education, the Republic of Indonesia

REFERENCES

[1] Maulidiyah, Nurdin M., Erasmus, Wibowo D., Natsir M., Ritonga H., Watoni A.H. 2015. Probe design of chemical oxygen demand (COD) based on photoelectrocatalytic and study of photocurrent formation at SnO-F/TiO_2 thin layer by using amperometry method. *International Journal of ChemTech Research,* 8(1):416-423.

[2] Nurdin M., Wibowo W., Supriyono, Febrian M.B., Surahman H., Krisnandi Y.K., Gunlazuardi J. 2009. Pengembangan metode baru penentuan *chemical oxygen demand* (COD) berbasis sel fotoelektrokimia: karakterisasi elektroda kerja lapis tipis TiO_2/ITO. *Makara, sains,* 13(1):1-8.

[3] Kim Y-C., Lee K-H., Sasaki S., Hashimoto K., Ikebukuro K., Karube I. 2000. Photocatalytic Sensor for chemical oxygen demand determination based on oxygen electrode. *Analytical Chemistry,* 72(14):3379-3382.

[4] Zhao H., Jiang D., Zhang S. 2004. Development of A Direct Photoelectrochemical Method for Determination of Chemical Oxygen Demand. *Analytical Chemistry*, 76:155-160.

[5] Nurdin M. 2014. Preparation, characterization and photoelectrocatalytic activity of Cu@N-TiO_2/Ti thin film electrode. *International Journal of Pharma and Bio Sciences,* 5(3):360-369.

[6] Maulidiyah, Ritonga H., Salamba R., Wibowo D., Nurdin M. 2015. Organic compound rhodamine B degradation by TiO_2/Ti electrode in a new portable reactor. *International Journal of ChemTech Research,* 8(6):645-653.

[7] Maulidiyah, Nurdin M., Wibowo D., Sani A. 2015. Nanotube titanium dioxide/titanium electrode fabrication with nitrogen and silver metal doped anodizing method: performance test of organic compound rhodamine B degradation. *International Journal of Pharmacy and Pharmaceutical Sciences,* 7(6):141-146.

[8] Nurdin M., Maulidiyah, Watoni A.H., Abdillah N., Wibowo D. 2016. Development of extraction method and characterization of TiO_2 mineral from ilmenite. *International Journal of ChemTech Research,* 9(4):483-491.

[9] Nurdin M., Zaeni A., Maulidiyah, Natsir M., Bampe A., Wibowo D. 2016. Comparison of conventional and microwave assisted extraction methods for TiO_2 recovery in mineral sands. *Oriental Journal of Chemistry,* 32(4):xx-xx.

[10] Nurdin M., Muzakkar M.Z., Nurjannah, Maulidiyah, Wibowo D. 2016. Plasmonic Silver-N/TiO_2 effect on photoelectrocatalytic oxidation reaction. *Journal of Environmental and Materials Science,* 7(9):xx-xx.

[11] Maulidiyah, Tribawono D.S., Wibowo D., Nurdin M. 2016. Electrochemical profile degradation of amino acid by flow system using TiO_2/Ti nanotubes Electrode. *Analytical & Bioanalytical Electrochemistry,* 8(6):xx-xx

[12] Fujisima A., and Honda K. 1972. Electrochemical Photolysis of Water at A Semoconductor Electrode. *Nature,* 238, 37-38.

[13] Nurdin M., and Maulidiyah. 2014. Fabrication of TiO_2/Ti nanotube electrode by anodizing method and its application on photoelectrocatalytic system. *International Journal of Scientific & Technology Research,* 3(2):122-126.

[14] Maulidiyah, Ritonga H., Faiqoh C.E., Wibowo D., Nurdin M. 2015. Prepration of TiO_2-PEG thin film on hydrophilicity performance and photocurrent response. *Biosciences Biotechnology Research Asia,* 12(3):1985-1989.

[15] Maulidiyah, Wibowo D., Hikmawati, Salamba R., Nurdin M. 2015. Preparation and characterization of activated carbon from coconut shell-doped TiO_2 in water medium. *Oriental Journal of Chemistry,* 31(4):2337-2342.

[16] Verbruggen S.W. 2015. TiO_2 photocatalysis for the degradation of pollutants in gas phase: from morphological design to plasmonic enhancement. *Journal of Photochemistry and Photobiology C: Photochemistry Reviews,* 25:64-82.

[17] Neppolian B., Mine S., Horiuchi Y., Bianchi C.L., Matsuoka M., Dionysiou D.D., Anpo M. 2016. Efficient photocatalytic degradation of organics present in gas and liquid phases using Pt-TiO_2/Zeolite (H-ZSM). *Chemosphere,* 153:237-243.

[18] Deng Q.R., Xia X.H., Guo M.L., Gao Y., Shao G. 2011. Mn-doped TiO_2 nanopowders with remarkable visible light photocatalytic activity. *Materials Letters,* 65:2051-2054.

[19] Maddila S., Ndabankulu V.O., Jonnalagadda S.B. 2016. Photocatalytic ozonation for degradation of tetradifon pesticide on Mn/TiO_2 under visible light. *Global NEST Journal,* 18(2):269-278.

[20] Ma X., and Chen Y. 2015. Preparation and characterization of Mn/N co-doped TiO_2 loaded on wood-based activated carbon fiber and its visible light photodegradation. *Polymers,* 7:1660-1673.

[21] Zhao Y.F., Li C., Lu S., Liu R.X., Hu J.Y., Gong Y.Y., Niu L.Y. 2016. Electronic, optical and photocatalytic behavior of Mn, N doped and co-doped TiO_2: experiment and simulation. *Journal of Solid State Chemistry,* 235:160-168.

[22] Ruslan, Wahab A.W., Nafie N.L., Nurdin M. 2013. Synthesis and characterization of electrodes N-TiO_2/Ti for chemical oxygen demand sensor with visible light response flow. *International Journal of Scientific & Technology Research,* 2(12):220-224.

[23] Maulidiyah, Nurdin M., Widianingsih E., Azis T., Wibowo D. 2015. Preparation of visible photocatalyst N-TiO_2 and its activity on congo red degradation. *ARPN Journal of Engineering and Applied Sciences,* 10(15):6250-6256.

[24] Padmavathi D.A. 2011. Potential energy curves & material properties. *Materials Sciences and Applications,* 2:97-104.

[25] Jeng M-J., Wung Y-L., Chang L-B., Chow L. 2013. Particle size effects of TiO_2 layers on the solar efficiency of dye-sensitized solar cells. *International Journal of Photoenergy,* 2013:1-9.